Pattern Recognition Letters 31 (2010) 83–90

Contents lists available at ScienceDirect

Pattern Recognition Letters

journal homepage: www.elsevier.com/locate/patrec

Quasi-automatic initialization for parametric active contours

C. Tauber *, H. Batatia, A. Ayache

IRIT-ENSEEIHT, 2 Rue Camichel BP 7122, F-31071 Toulouse, France

ARTICLE INFO

Article history:
Received 11 December 2007
Received in revised form 29 May 2009
Available online 21 August 2009

Communicated by H.H.S. Ip

Keywords:
Automatic initialization
Segmentation
Active contours
Gradient vector flow

ABSTRACT

Active contour is a well-known image segmentation technique, commonly used to find object boundaries in images. Its main benefit is its ability to retrieve an ordered collection of points. However, fitting precisely a deformable contour to actual boundaries depends strongly on its initialization and requires adjusting various parameters.

This paper presents an original method to initialize quasi-automatically explicit deformable models when segmenting regions that require no change of topology. The proposed method relies on a careful study of the gradient vector flow. Two original concepts are introduced, namely strong and weak divergence centers. The analysis of the properties of these centers leads to establishing a quasi-automatic method to setup an initial curve that will reach all the boundaries of a target region. Results using synthetic and real images are presented, showing the validity of our approach.

1. Introduction

Active contours (Kass et al., 1988), or snakes, are dynamic curves that evolve within an image domain to reach an optimal position and shape by minimizing an energy functional. Usually, they require an initial contour close to the target image feature. Since their introduction, numerous methods have been developed attempting to improve the performance of the parametric snakes (Chakraborty et al., 1996; Chan and Vese, 2001; Delingette and Montagnat, 2000; Jehan-Besson et al., 2003; McInerney and Terzopoulos, 1995; Ronfard, 1994; Staib and Duncan, 1992).

The aim of this paper is to address one major limitation of explicit variational methods: their sensitivity to initialization, which has a significant impact on the results. We limit the study to regions that can be segmented with one explicit active contour, without topological change.

Traditional active contours do not have large capture range due to the rapid decrease of their external forces as the distance to the object contour increases. In order to obtain an acceptable solution, the initial contour must therefore be very close to the desired object contour. To our knowledge, there is currently no fully automatic method to initialize active contours without strong a priori knowledge on what is segmented (Gerard and Makram-Ebeid, 1998; Lefebvre et al., 1998; Moursi and El-Sakka, 2008). Some methods, however, have contributed to facilitate the parametric snake initialization in a general framework. Cohen introduced the balloon snakes (Cohen, 1991). He considers the snake as an inflated balloon. A pressure force is added to the interior to push it towards the desired contour. This method facilitates the initialization and also helps to overpass local energetical minima caused by noise. However, it introduces an additional parameter which controls the pressure force and the balance between overpassing local extrema and stopping at actual edges. The setup of this parameter is not easily amenable to automatization. Xu and Prince (1998) proposed the gradient vector flow (GVF). The GVF is computed as the diffusion of gradient vectors of a gray level image. This external force, when added to a snake, extend the capture range of region boundaries, permitting more flexible initialization. However, while this model is less sensitive to the distance between the initial curve and the target boundaries, we demonstrate in Section 2.2 that the result strongly depends on the position of the initial curve within the gradient vector flow field.

In this paper, we study the properties of the gradient vector flow and contribute to solve its sensitivity to initial positioning of the curve. This leads to present an original quasi-automatic initialization method for GVF snakes. Our method does not rely on any a priori knowledge except that no topological change is needed to segment the region. In addition to its effectiveness, we show that our method can be generalized to initialize non GVF-based snakes.

The remainder of this paper is organized as follows. Section 2 describes the GVF method and its limitation for snake initialization. The new concept of centers of divergence is defined in Section 3 and its properties are analysed. In Section 4, we establish a fundamental property that must be verified by the initial curve and propose our quasi-automatic initialization method. Results on synthetic and real images are shown and discussed in Section 5. Finally, Section 6 draws some conclusions.

* Corresponding author.
E-mail addresses: tauber@enseeiht.fr (C. Tauber), batatia@enseeiht.fr (H. Batatia), ayache@enseeiht.fr (A. Ayache).

0167-8655/$ - see front matter © 2009 Elsevier B.V. All rights reserved.
doi:10.1016/j.patrec.2009.08.010

2. The gradient vector flow

2.1. The GVF model

A snake is a curve that evolves from an initial position towards the boundary of an object, minimizing an energy functional (Kass et al., 1988). The functional consists of two terms: internal energy and external energy. The first term affects the smoothness of the curve, while the second attracts the snake toward image features. Most of the external energies proposed in the literature use either gradient information or global image statistics. The gradient vector flow is an external energy introduced by Xu and Prince (1998). It has the inherent property of being able to reconstruct subjective contours and partially solve the initialization problem.

The gradient vector flow field is the vector field $\boldsymbol{v}(x,y) = [u(x,y), v(x,y)]$ that minimizes the following energy functional

$$E = \iint \mu(u_x^2 + u_y^2 + v_x^2 + v_y^2) + |\nabla f|^2 |\boldsymbol{v} - \nabla f|^2 dxdy, \tag{1}$$

where u_x, u_y, v_x and v_y are the partial derivatives and μ is a regularization parameter. $f(x,y)$ is an edge map derived from the image $I(x,y)$ having the property that it is larger near image edges. The first term of the functional predominates in areas where the information is constant, giving a smooth flow map in homogeneous regions. The second term takes over when there are strong variations, leading to $\boldsymbol{v} = \nabla f$ near boundaries.

Using the calculus of variation, the GVF can be determined by solving the Euler equations:

$$\mu\nabla^2 u - \left(u - \frac{\partial f}{\partial x}\right)\left(\frac{\partial f^2}{\partial x} + \frac{\partial f^2}{\partial y}\right) = 0, \tag{2}$$

$$\mu\nabla^2 v - \left(v - \frac{\partial f}{\partial y}\right)\left(\frac{\partial f^2}{\partial x} + \frac{\partial f^2}{\partial y}\right) = 0. \tag{3}$$

2.2. Instability against initial curve

As presented in (Xu and Prince, 1998), the GVF attracts the snake to the contours, even if it is far away. However, this does not completely solve the initialization problem. In Fig. 1, the first row is an example reproduced from (Xu and Prince, 1998), where the GVF is successfully used to segment the region from a far initialization. In the bottom row, we show the segmentation of the same image with the same algorithm, but with the initial curve slightly shifted to the left. The result is totally different: the snake is crushed against one side of the boundary. This phenomenon repeats whenever the initial curve does not surround the center of the shape. We will show in the following sections the reasons of this behaviour.

3. The centers of divergence

In order to explain the failure of the GVF model, a fine analysis is needed. For this purpose, we define the concept of strong and weak centers of divergence.

3.1. Definition

Intuitively, in Fig. 1, to correctly segment the shape, the initial curve has to surround the *center* of the field. This was first noticed in (Xingfei and Tian, 2002). To handle complex shaped regions, we generalize the notion of center of divergence. We define the centers of strong divergence and the centers of weak divergence. Our quasi-automatic initialization of the snake is based on these two new concepts.

Let $\text{sign}(x)$ be a function indicating the sign of x:

$$\text{sign}(x) = \begin{cases} 1 & x > 0 \\ 0 & x = 0 \\ -1 & x < 0 \end{cases} \tag{4}$$

Let $\boldsymbol{v}(i,j) = (u(i,j), v(i,j))$ be the GVF. For the remaining of the paper, the GVF is supposed non nil everywhere in the image domain. In practice, this can always be achieved given any non-constant edge map. This is because the GVF is calculated as a generalized diffusion of the gradient vectors of the edge-map. By choosing an appropriate diffusion time, we can ensure that all vectors in the field have a positive norm.

We define $\mathscr{C}_h$ and $\mathscr{C}_v$ as:

$$\mathscr{C}_h = \{(i,j) | u(i,j) \leqslant u(i,j+1) \wedge abs(\text{sign}(u(i,j)) + \text{sign}(u(i,j+1))) \leqslant 1\}, \tag{5}$$

$$\mathscr{C}_v = \{(i,j) | v(i,j) \leqslant v(i+1,j) \wedge abs(\text{sign}(v(i,j)) + \text{sign}(v(i+1,j))) \leqslant 1\}. \tag{6}$$

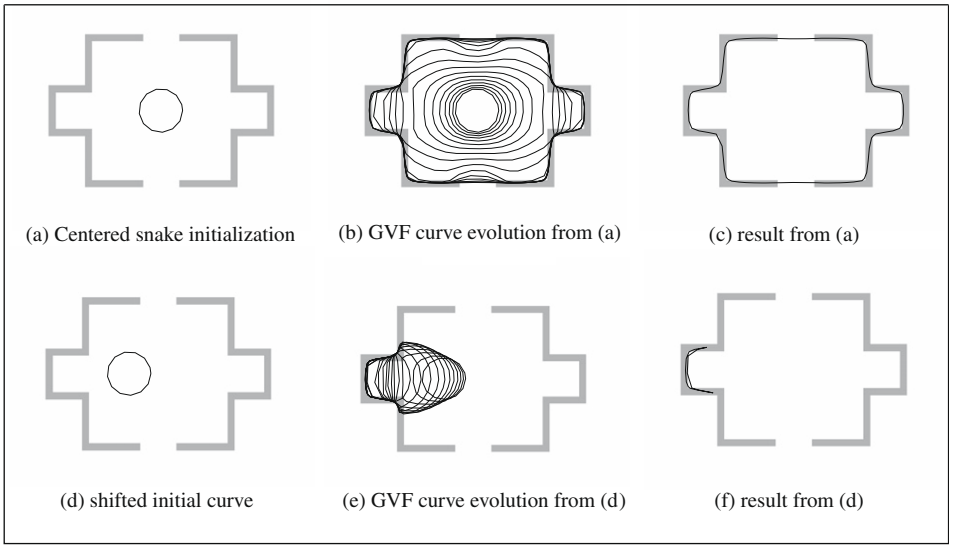

Fig. 1. Effect of the initialization. (a–c) Reproduced experimentation from (Xu and Prince, 1998). (d–f) Same method after shifting slightly the initial curve.

$\mathscr{C}_h$ is the set of points (i,j) in the field where the vectors $\boldsymbol{v}(i,j)$ are diverging horizontally. It corresponds to the points where the horizontal component $u(i,j)$ of $\boldsymbol{v}(i,j)$ is negative and $u(i,j+1)$ is positive. $\mathscr{C}_v$ is the set of points (i,j) in the field where the vectors $\boldsymbol{v}(i,j)$ are diverging vertically. It corresponds to the points where the vertical component $v(i,j)$ of $\boldsymbol{v}(i,j)$ is negative and $v(i+1,j)$ is positive.

We define the centers of strong and weak divergence from these two equations. We denote $\boldsymbol{Cd}_{\text{strong}}$ the set of centers of strong divergence, and $\boldsymbol{Cd}_{\text{weak}}$ the set of centers of weak divergence of the GVF:

$$\boldsymbol{Cd}_{\text{strong}} = \{(i,j)|(i,j) \in \mathscr{C}_h \ \wedge \ (i,j) \in \mathscr{C}_v\}, \tag{7}$$

$$\boldsymbol{Cd}_{\text{weak}} = \{(i,j)|(i,j) \in \mathscr{C}_h \ \vee \ (i,j) \in \mathscr{C}_v\}. \tag{8}$$

The centers of weak divergence are the points where the vectors of the GVF diverge in one (either horizonal or vertical) direction. The centers of strong divergence feature both horizontal and vertical divergences. An example of the $\boldsymbol{Cd}_{\text{strong}}$ and $\boldsymbol{Cd}_{\text{weak}}$ is presented in Fig. 2. The $\boldsymbol{Cd}_{\text{strong}}$ of the shown field is in white and the $\boldsymbol{Cd}_{\text{weak}}$ are in gray; other points from the field are in black. Note that all directions of GVF vectors of all neighbours of the $\boldsymbol{Cd}_{\text{strong}}$ are receding from it.

Fig. 3 shows examples of $\boldsymbol{Cd}_{\text{strong}}$ and $\boldsymbol{Cd}_{\text{weak}}$ calculated on a synthetic image.

3.2. Analysis of the centers of divergence

The centers of weak divergence form paths, whose intersections are the centers of strong divergence. Fig. 4 shows the center of strong divergence of the *room* image. In this simple case, the initial curve has to include the $\boldsymbol{Cd}_{\text{strong}}$ in order to converge correctly toward the contours. We generalize this property for complex non-symmetric and non-convex shapes in Section 4.1.

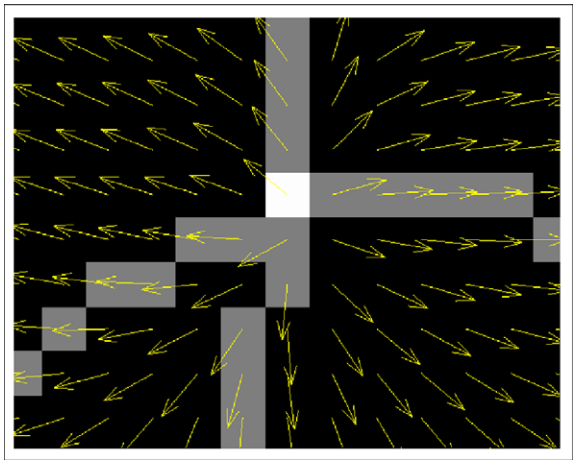

Fig. 2. Zoom on a GVF field and its corresponding center of strong divergence (white) and centers of weak divergence (gray).

3.2.1. Critical path

We call critical path any path of adjacent centers of weak divergence connecting some centers of strong divergence. The GVF of an image may feature several critical path (see Fig.3c).

3.2.2. Properties of critical paths and centers of divergence

3.2.2.1. Property 1: In a GVF, all vectors of the neighbours of a centre of strong divergence c recede from it. This property is illustrated on Fig. 5, and can be formalized as follows:

$$\forall p \in \mathscr{V}_{\text{orth}}(c): \ \vec{\boldsymbol{v}}(p) \cdot \vec{\omega} \geqslant 0, \tag{9}$$

$$\forall p \in \mathscr{V}_{\text{diag}}(c): \ u(p)\omega_i \geqslant 0 \ \vee \ v(p)\omega_j \geqslant 0, \tag{10}$$

where $\vec{\omega} = \vec{cp} = (\omega_i, \omega_j)$; $\mathscr{V}_{\text{orth}}(c)$ is the set of neighbours of c in horizontal and vertical directions ($\{v_2, v_4, v_6, v_8\}$ in Fig. 5); and $\mathscr{V}_{\text{diag}}(c)$ is the set of neighbours of c in diagonal directions ($\{v_1, v_3, v_5, v_7\}$ in Fig. 5). $\mathscr{V}_{\text{orth}}(c) \bigcup \mathscr{V}_{diag}(c)$ forms the 8-connexity neighbourhood of c.

Let $c = (i,j) \in \boldsymbol{Cd}_{\text{strong}}$. According to the $\boldsymbol{Cd}_{\text{strong}}$ definition:

- $u(i,j) < 0$;
- $u(i,j+1) \geqslant 0$;
- $v(i,j) < 0$;
- $v(i+1,j) \geqslant 0$.

Lets consider the horizontal component of the vector $\boldsymbol{v}(c) = (u(i,j), v(i,j))$ of this $\boldsymbol{Cd}_{\text{strong}}$: by definition $u(i,j) < 0$. Suppose that (i,j) and $(i-1,j)$ do not belong to a contour, which is legitimate for regions where the distance between two opposite boundaries is superior to two pixels, then $u(i,j-1) < 0$. The opposite would mean that one of these points is on a contour, because we can ensure that the only convergent vectors are associated to points on contours by controlling the GVF homogeneity. Moreover, the vector field is defined on a discrete grid and thus a contour cannot pass between two points if none of them is on the contour. In the same way, we show that $v(i-1,j) \leqslant 0$ since $v(i,j) < 0$.

Using notations from Fig. 5, the divergence of neighbours $\mathscr{V}_{\text{diag}}$ is also ensured by homogeneity constraints of the field. Suppose again that neighbours of the central pixel c are not on a contour. If one of the points v_1, v_3, v_5 et v_7 have both its directional components in the direction of c, it does not minimize the second term of the functional (Eq. (1)). Considering the orientation of the neighbours, the vector with opposite direction would reduce the energy of the field.

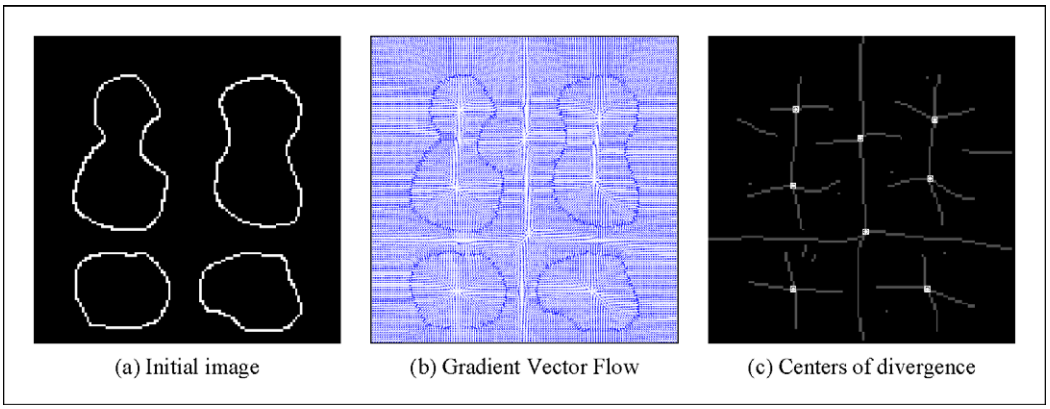

Fig. 3. GVF and centers of weak (gray) and strong (white) divergence of a synthetic image.

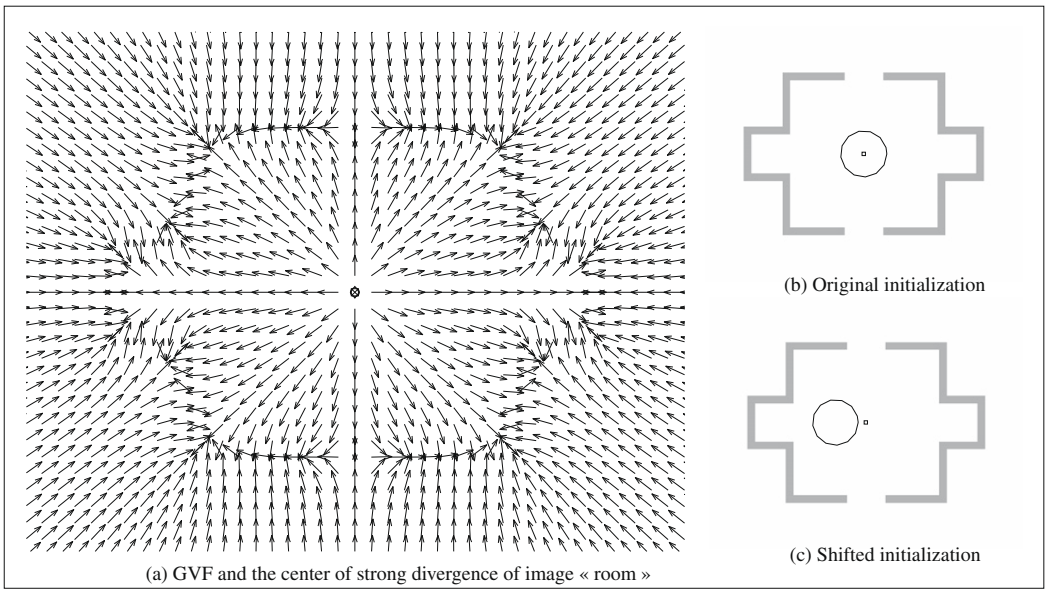

Fig. 4. GVF and initializations of the *room* image.

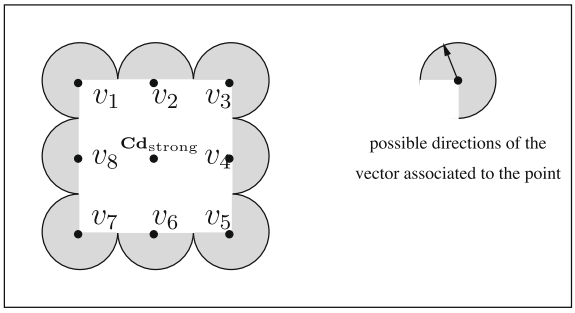

Fig. 5. Possible directions of GVF vectors in the neighbourhood of a $\boldsymbol{Cd}_{\mathrm{strong}}$.

3.2.2.2. Property 2: Any closed homogeneous region bounded by the image contours has one and only one critical path. The existence of the critical path is obvious. The vectors of the GVF near the contours inside a closed region point towards these contours. Opposite vertical and horizontal contours thus imply the existence of vectors diverging horizontally and vertically. By construction, at least one point within the region has thus to be a $\boldsymbol{Cd}_{\mathrm{strong}}$, which constitute a critical path by itself.

Lets consider a closed homogeneous region that has several distinct critical paths. By construction, the vectors between two critical paths are converging, implying the presence of a contour. Let's study the extremities of this contour. On one hand, if the extremities of this contour both reach the external contour of the region, then it splits the considered region into two distinct regions. On the other hand, if one extremity of the contour does not reach the external contour of the region, then by construction it exists a path of adjacent centers of weak divergence that passes between the external contour and the extremity, connecting the two critical paths.

4. Automatic initialization

4.1. Fundamental property of initialization

Considering the previous properties, we establish the following proposition.

An active contour based on any GVF energy evolves to a region boundary if the initial curve satisfies the following conditions:

- *it is totally included in the region to be segmented;*
- *it surrounds the critical path of the region; in other words, it surrounds all centers of strong divergence of the region, and all the centers of weak divergence connecting these* $\boldsymbol{Cd}_{\mathrm{strong}}$.

These conditions are sufficient in order for the curve to be attracted towards all parts of the boundary. By construction, the curve will further apart the centers of divergence in all directions. Suppose that the curve is not attracted by a part of the contour of the region. This means that there is a part of the region that the curve does not reach. The vectors inside this part are thus receding its center. This center is a $\boldsymbol{Cd}_{\mathrm{strong}}$. However, such a center would have been inside the curve by construction.

Starting from inside the region is not mandatory as it is sometime acceptable to start from outside. However, it brings several advantages. First, when the initial curve is outside the region, we cannot ensure that the curve will not be attracted by contours from other regions without knowing which contours corresponds to which region. Second, the inside of a region generally has some homogeneity properties (e.g. intensity, texture) that can be used in a pre-filtering process of the image to improve the GVF quality.

For automatization purposes, we thus suppose that the initial curve should preferably be inside the region to segment. We show that the other condition is then necessary. There are two situations where this condition would not be respected: (1) the initial curve does not surround one or several centers of strong divergence of the region, (2) the initial curve does not surround all the centers of weak divergence that connect the centers of strong divergence of the region. Let's consider each of these options:

- In the first option, the property of the receding neighbours of the centers of strong divergence guaranties that any of them left out will repulse the snake. The final curve would therefore not include these centers. Some parts of the region would not be segmented.
- In the second option, the curve would cross over the path of the centers of weak divergence. At the intersection, the parts of the curve on each side of the path will evolve in opposite directions

and reach opposite boundaries. The segmentation would not fit the shape of the contour.We illustrate this property in Fig. 8c1–c4.

4.2. Automatic initialization algorithm

From the fundamental proposition of initialization, we propose a method for automatic initialization of the snake. This algorithm first considers an arbitrary point inside the region to segment. The property of the receding directions can be used in the opposite way: if we inverse the GVF, all the vectors are converging toward one or several $\boldsymbol{Cd}_{\text{strong}}$ (Fig. 6). From the initial point, we follow the inverse GVF directions to reach a pixel in $\boldsymbol{Cd}_{\text{strong}}$:

While $(p \notin \boldsymbol{Cd}_{\text{strong}})$
  $p \leftarrow (p - \boldsymbol{v}(p))$
EndWhile

Once a point $p_s \in \boldsymbol{Cd}_{\text{strong}}$ is found, we select all the $\boldsymbol{Cd}_{\text{strong}}$ connected to it via $\boldsymbol{Cd}_{\text{weak}}$ points. We use a morphological operator to dilate the connected path and we extract its boundary. This boundary is the seeked initial curve. This method ensures that the curve complies with our fundamental property of initialization.

Fig. 7 presents the automatic initialization of the image shown in Fig. 8. An arbitrary point has been manually selected inside the region. Following the inverse GVF, the route to one $\boldsymbol{Cd}_{\text{strong}}$ of the region has been found (star line). The initial curve is in dashed line. In order to make the initial curve smooth, we create a B-spline interpolation of it (control points shown as circles).

This method can be used to segment any closed shape. In image sequences, the resulting curve of the previous frame cannot be used directly to initialize the snake in the current frame, as the curve has to be strictly included in the region to be segmented. However, for moderate motions, the barycenter of the previous result can be used as the startup point for the initialization in the current frame.

4.3. Generalized initialization method

The initialization can be generalized to active contours that are not based on the GVF. We propose to include an additional static external force term into the snake framework. This additional force term is an inhibited gradient vector flow that is used to initialize the curve and expand it toward the boundaries. We first normalize the GVF:

$$\boldsymbol{v}_N(x,y) = \frac{\boldsymbol{v}(x,y)}{\sqrt{|u(x,y)|^2 + |v(x,y)|^2}}, \tag{11}$$

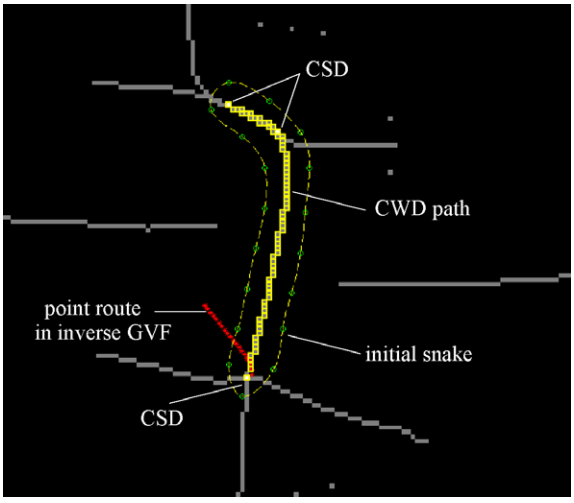

Fig. 7. Automatic initialization of a snake using the centers of strong and weak divergence of the GVF.

where $\boldsymbol{v}_N(x,y)$ is the normalized GVF at (x,y).

We want the new energy force to attract the curve close to the contour, but without overriding the other snake external energy term. Therefore we propose *an inhibition function*. First we generate the map $\mathscr{R}$ of the distances to the contours. The contour map is noted I_c, and can be determined coarsely.

$$\mathscr{R}(p=(i,j)) = \min_{q \in I_c^+} \|p - q\|, \tag{12}$$

where I_c^+ is the set of contours pixels in I_c. The inhibition map $\Xi(i,j)$ is precomputed as a modified Tukey's function:

$$\Xi(i,j) = \begin{cases} \frac{3\mathscr{R}(i,j)^2}{\varsigma^2} - \frac{3\mathscr{R}(i,j)^4}{\varsigma^4} + \frac{\mathscr{R}(i,j)^6}{\varsigma^6} & \text{if } \mathscr{R}(i,j) \leqslant \varsigma, \\ 1 & \text{otherwise.} \end{cases} \tag{13}$$

where ς is the inhibition parameter. ς sets the minimal distance above which the GVF is not inhibited. The inhibited GVF is used to automatically generate the initial curve as well as expand it towards the contours.

5. Experimentations

5.1. Synthetic contours

Fig. 8 illustrates the effect of our automatic initialization compared to three others. Fig. 8A shows the initial image

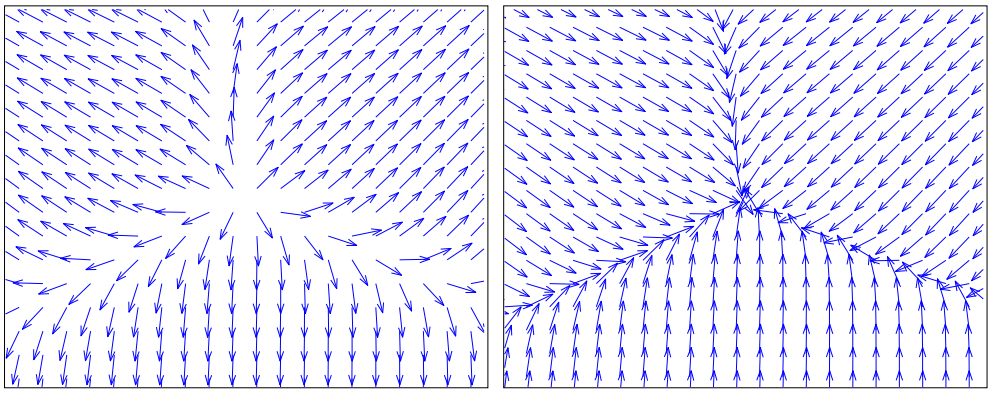

(a) GVF (b) Inverse GVF

Fig. 6. Inverse gradient vector flow.

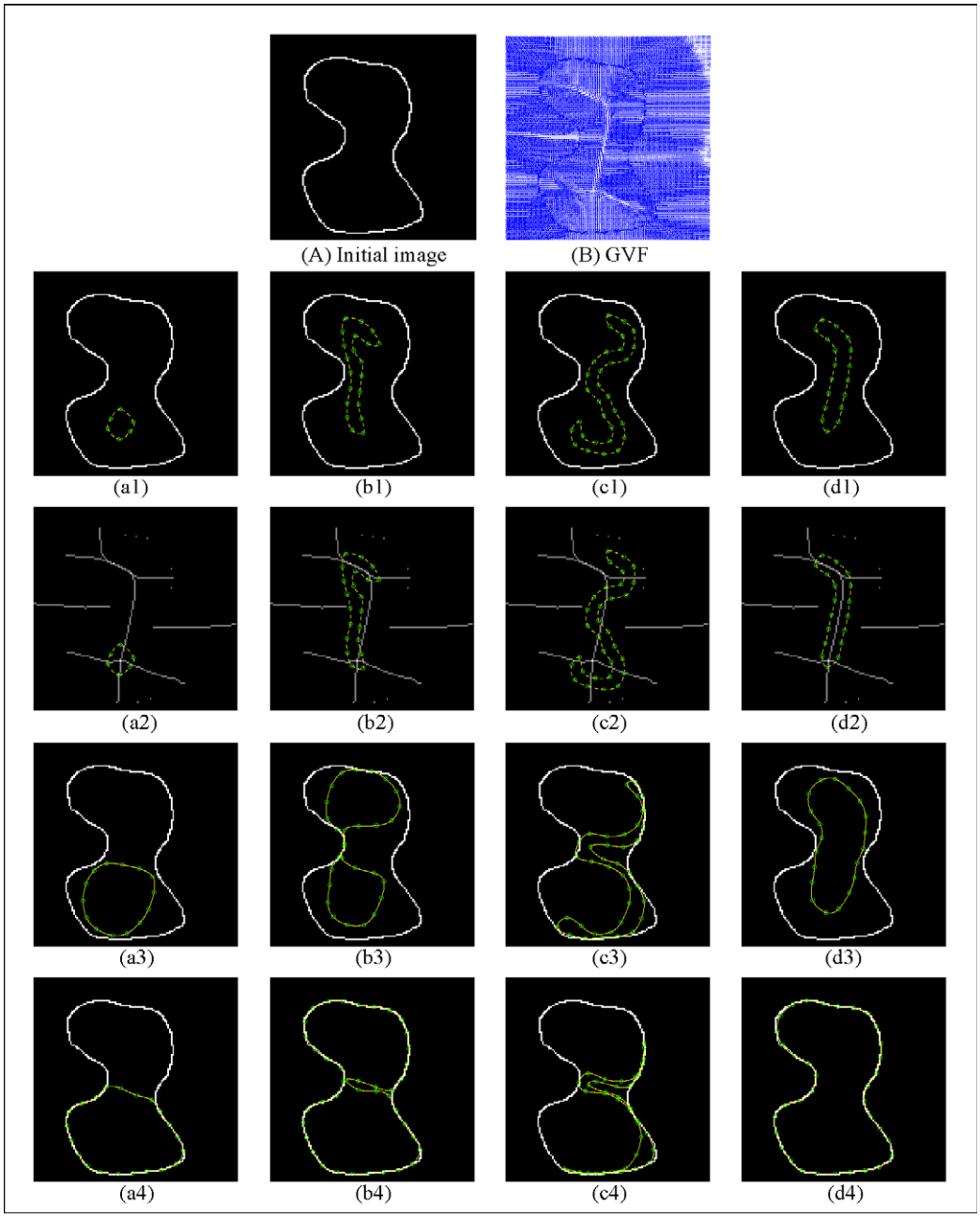

Fig. 8. GVF Snake evolution from different initializations.

with the shape to be segmented. Fig. 8B shows the corresponding GVF. The four columns show the different initializations.

- Column (a): the initial curve contains only one of the three centers of strong divergence of the region.
- Column (b): the initial curve contains the three $\boldsymbol{Cd}_{\text{strong}}$ but not all the $\boldsymbol{Cd}_{\text{weak}}$ connecting them.
- Column (c): the initial curve contains no $\boldsymbol{Cd}_{\text{strong}}$ but covers a significant surface of the region.
- Column (d): the initial curve respects our fundamental initialization proposition.

Rows of the Fig. 8 illustrate different stages of the segmentation:

- line (1) presents the initial curve;
- line (2) shows the location of the initial curve with regard to the $\boldsymbol{Cd}_{\text{strong}}$ and $\boldsymbol{Cd}_{\text{weak}}$;
- line (3) is an iteration during the segmentation process;
- line (4) shows the final results of the segmentation.

We clearly notice that the results fully comply with proposition 4.1:

(1) with initialization (a), the snake stops at half-height of the region. It cannot go further because the centers of divergence of the superior part of the region hold it back.
(2) with initialization (b), the final snake fits the contour, however, one part of the curve degrades the result. It corresponds to the location where the initial curve crosses the critical path.
(3) with initialization (c), the final snake is crushed against one side of the contour, similarly to initialization (b).

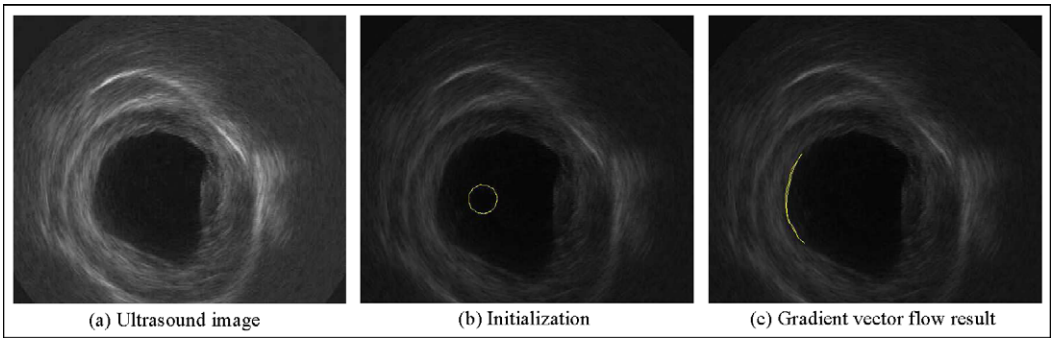

Fig. 9. Segmentation result with arbitrary initialization.

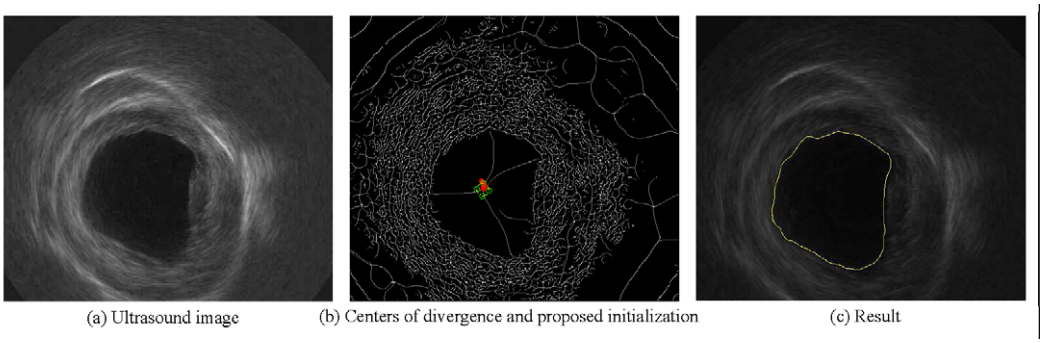

Fig. 10. Segmentation result with our automatic initialization.

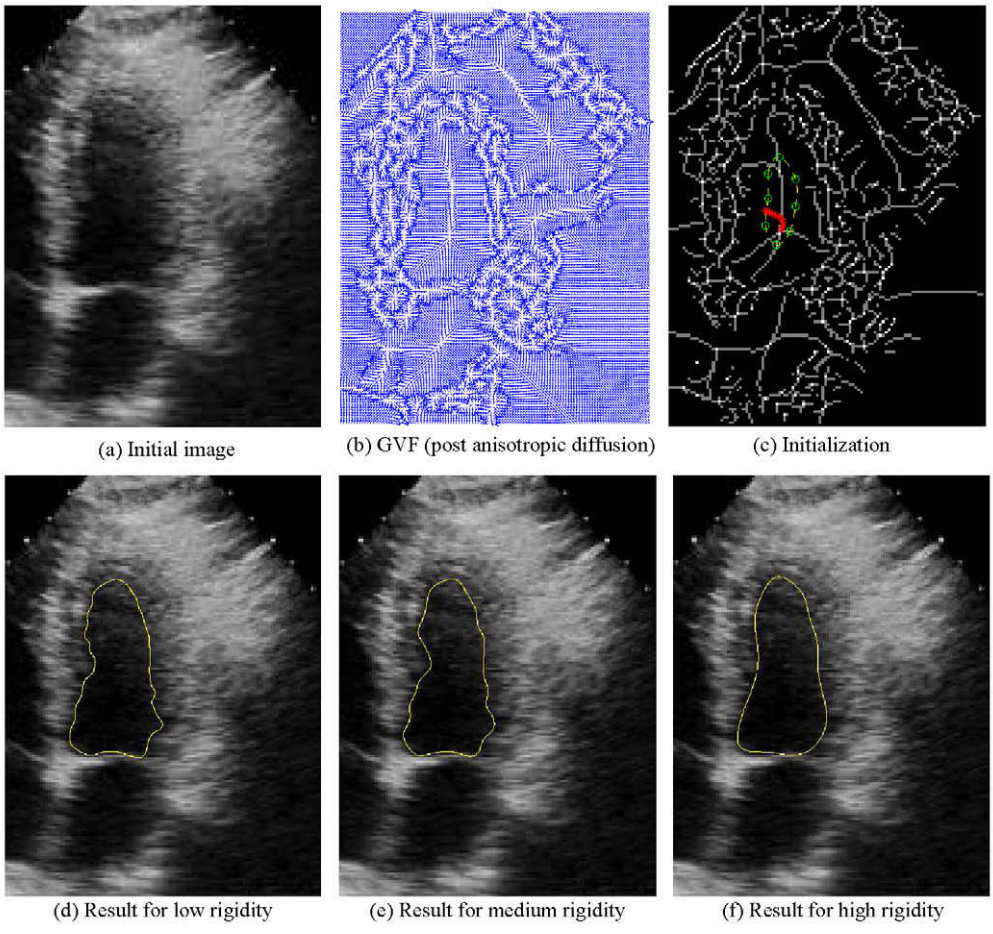

Fig. 11. Segmentation result of a left ventricle with our automatic initialization.

(4) initialization (d) does not seem significantly different from initialization (b). Moreover, it is farther from the contours than initialization (c). However, it is the only one that leads to an acceptable segmentation.

5.2. Real ultrasound images

In this section we present comparative segmentation results with our automatic initialization and other arbitrary methods, on ultrasound images. For a better visibility, the dynamic range of the intensity of the initial image has been mapped to $[[0, 127]]$ when curves are displayed. We used the GVF of Xu and Prince with an edge map equal to the local coefficient of variation, as it is well adapted to detect edges in ultrasound images (Tauber et al., 2009).

Fig. 9a shows an endocorporal ultrasound image. Fig. 9b shows an initialization that does not verify our fundamental conditions. Fig. 9c shows the result of the segmentation. The snake is again crushed against one side of the heart cavity.

Fig. 10 shows the map of the centers of strong and weak divergence and the corresponding automatic initialization. With this initial curve, the left ventricle was correctly segmented, even though the initialization is far from the boundaries (Fig. 10c).

We used our initialization method to segment another echocardiographic image (Fig. 11a). The acquisition frequency is lower than with the endocorporal transducer, leading to a lower resolution. The image has thus first been filtered out using a robust speckle reducing anisotropic diffusion (Tauber et al., 2004). The region has several centers of strong divergence. The gradient vector flow subsequently computed is shown in Fig. 11b. The initialization stages and the resulting initial curve are shown in Fig. 11c. Finally three different segmentation results using the GVF with an edge-map equal to the coefficient of variation are presented in Fig. 11d–f. Each one correspond to a different elasticity parameter of the snake. All three fit correctly the snake to the boundary of the ventricle.

6. Discussion and conclusions

In this paper we presented the concepts of centers of strong and weak divergence. From their properties, we derived a new method to initialize any active contour. This method is quasi-automatic as it only requires the selection of one arbitrary point in the target region. We proposed an inhibited GVF force that can be added to any active contour to allow its automatic initialization towards the object boundaries. The experimental results on synthetic and echocardiographic images show the effectiveness of the method. Current work target the adaptation on this method to 3D models. An adaptation to allow segmenting regions that feature topological changes will be proposed.

Acknowledgements

We thank the reviewers for their helpful comments.

References

Chakraborty, A., Staib, L.H., Duncan, J.S., 1996. Deformable boundary finding in medical images by integrating gradient and region information. IEEE Trans. Med. Imaging 15, 859–870.

Chan, T.F., Vese, L.A., 2001. Active contour without edges. IEEE Trans. Image Process. 10, 266–277.

Cohen, L., 1991. On active contour models and balloons. Comput. Vision Graphics Image Process.: Image Understanding 53, 211–218.

Delingette, H., Montagnat, J., 2000. Shape and topology constraints on parametric active contours. Comput. Vision Image Understanding 83, 140–171.

Gerard, O., Makram-Ebeid, S., 1998. Automatic contour detection by encoding knowledge into active contour models. In: Proc. 4th IEEE Workshop on Applications of Computer Vision (WACV98), pp. 115–120.

Kass, M., Witkin, A., Terzopoulos, D., 1988. Snakes: Active contour models. Internat. J. Comput. Vision 1, 321–332.

Jehan-Besson, S., Barlaud, M., Aubert, G., 2003. DREAM2S: Deformable regions driven by an Eulerian accurate minimization method for image and video segmentation. Internat. J. Comput. Vision 53, 45–70.

Lefebvre, F., Berger, G., Laugier, P., 1998. Automatic detection of the boundary of the calcaneus from ultrasound parametric images using an active contour model. IEEE Trans. Med. Imaging 17, 45–52.

McInerney, T., Terzopoulos, D., 1995. T-snakes: Topologically adaptive snakes. Med. Image Anal. 4, 73–91.

Moursi, S.G., El-Sakka, M.R., 2008. Active contours initialization for ultrasound carotid artery images. In: Proc. IEEE/ACS Internat. Conf. on Computer Systems and Applications, pp. 629–636.

Ronfard, R., 1994. Region-based strategies for active contour models. Int. J. Comput. Vision 13, 229–251.

Staib, L.H., Duncan, J.S., 1992. Boundary finding with parametrically deformable models. IEEE Trans. Pattern Anal. Machine Intell. 14, 1061–1075.

Tauber, C., Batatia, H., Ayache, A., 2004. A robust speckle reducing anisotropic diffusion. In: IEEE Internat. Conf. on Image Processing (ICIP).

Tauber, C., Batatia, H., Ayache, A., 2009. Robust B-spline snakes for ultrasound image segmentation. J. Sign. Process. Syst. 54, 159–169.

Xingfei, G., Tian, J., 2002. An automatic active contour model for multiple objects. In: Proc. Internat. Conf. on Pattern Recognition, pp. 881–884.

Xu, C., Prince, J.L., 1998. Snakes, shapes, and gradient vector flow. IEEE Trans. Image Process. 7, 359–369.